Molecular and Cellular Biochemistry (2020) 474:229–241
https://doi.org/10.1007/s11010-020-03848-x

Dynamic regulation of histone H3 lysine (K) acetylation and deacetylation during prolonged oxygen deprivation in a champion anaerobe

Sanoji Wijenayake[1,2] · **Kenneth B. Storey**[1,3]

Received: 15 April 2020 / Accepted: 20 July 2020 / Published online: 29 July 2020

Abstract

Trachemys scripta elegans can survive up to three months of absolute anoxia at 3 °C and recover with minimal cellular damage. Red-eared sliders employ various physiological and biochemical adaptations to survive anoxia with metabolic rate depression (MRD) being the most prominent adaptation. MRD is mediated by epigenetic, transcriptional, post-transcriptional, and post-translational mechanisms aimed at shutting down cellular processes that are not needed for anoxia survival, while reprioritizing ATP towards cell processes that are vital for anaerobiosis. Histone acetylation/deacetylation are epigenetic modifications that maintain a proper balance between permissive chromatin and restricted chromatin, yet very little is known about protein regulation and enzymatic activity of the writers and erasers of acetylation during natural anoxia tolerance. As such, this study explored the interplay between transcriptional activators, histone acetyltransferases (HATs), and transcriptional repressors, sirtuins (SIRTs), along with three prominent acetyl-lysine (K) moieties of histone H3 in the liver of red-eared sliders. Western immunoblotting was used to measure acetylation levels of H3-K14, H3-K18, and H3-K56, as well as protein levels of histone H3-total, HATs, and nuclear SIRTs in the liver in response to 5 h and 20 h anoxia. Global and nuclear enzymatic activity of HATs and enzymatic activity of nuclear SIRTs were also measured. Overall, a strong suppression of HATs-mediated H3 acetylation and SIRT-mediated deacetylation was evident in the liver of red-eared sliders that could play an important role in ATP conservation as part of the overall reduction in metabolic rate.

Keywords Epigenetics · Anoxia · *T.s. elegans* · Histone lysine acetyltransferases · Sirtuins · Histone H3

Introduction

Freshwater turtles belonging to the *Chrysemys* and *Trachemys* genre are champion anaerobes that can survive approximately 90 days of continual anoxia at 3 °C and recover with minimal cellular injury [1–4]. Red-eared sliders (*Trachemys scripta elegans*) employ numerous well-adapted strategies to combat challenges that are associated with anaerobiosis, including (1) increase glycogen storage in liver, white skeletal muscle, and heart, (2) exclusively use anaerobic glycolysis to generate ATP [4–8], (3) buffer and store lactic acid (a byproduct of anaerobic glycolysis) in the shell [9–14], (4) enhance cytoprotection to combat against reactive oxygen species (ROS) [9, 15–19], and most importantly, (5) reduce the overall metabolic rate by 90% when compared to normoxia [2–5, 20, 21]. Although extensive work has already been done on the glycolytic controls [22–26], transcriptional [27–30], post-transcriptional [29, 31–33], and post-translational regulation [21, 34–36] involved in metabolic rate depression (MRD), epigenetic regulation of MRD, in particular, regulation of global gene expression through histone H3 lysine (K) modifications remains to be explored in red-eared sliders.

Reversible protein acetylation (RPA) of K moieties is one of the more well-studied epigenetic signatures mainly due to the discovery of more than 200 acetylated non-histone

✉ Kenneth B. Storey
Kenneth_storey@carleton.ca

[1] Department of Biology, Institute of Biochemistry, Carleton University, Ottawa, ON, Canada

[2] Present Address: Department of Biological Sciences and Center for Environmental Epigenetics and Development, University of Toronto, Toronto, ON, Canada

[3] Canada Research Chair in Molecular Physiology, Department of Biology, and Department of Chemistry, Institute of Biochemistry, 1125 Colonel By Drive, Ottawa, ON K1S 5B6, Canada

proteins, including metabolically relevant enzymes as well as transcription factors in mammals [37], along with the discovery of histone K acetyltransferases (HATs/KATs) and class I–IV histone deacetylases (HDACs) that work towards establishing a steady-state balance between transcriptional activation and repression of target promoters [38]. Histone K acetylation in particular is associated with transcriptional activation and promote an open-chromatin state [38–40], whereas histone deacetylation involves the removal of acetyl-moieties ($COCH_3$) that are covalently bound to K residues and is typically associated with transcriptional repression [41–43]. Both HATs and HDACs are capable of maintaining global as well as site-specific acetylation, and may function as a regulatory switch between repressive heterochromatin and permissive euchromatin [44]. In an environment where oxygen is limited or absent, this type of transcriptional regulation may be critical for silencing numerous genes that are not required for anoxia survival, while enhancing the expression of genes that are necessary in red-eared sliders.

HATs are grouped into six major families each with distinct function and target proteins. These include the Gcn5-related *N*-acetyltransferases (GNAT) superfamily [45, 46], the MYST family [47, 48], CBP/p300 [49, 50], the TBP-associated factor $TAF_{II}250$ and TFIID [51], members of the steroid receptor co-activators [52], and some gene-specific transcription factors including, ATF-2 and CIITA [53]. HDACs also can be divided into distinct families: class I including HDAC 1, 2, and 8, class II including HDAC 4, 5, 6, 7, 9, and 10, and class IV including HDAC11. However, class III HDACs consist of seven sirtuin (SIRTs) proteins that require NAD^+ as a cofactor to induce deacetylation [54]. Interestingly, HATs and HDACs are not limited to modifying only histone proteins, but also modify non-histone proteins that are part of metabolic regulation, cell cycle, apoptosis, DNA recombination, replication, and DNA repair [55, 56]. Transcription factors including p53 [57], HMG family of proteins [58], STAT3 [59], c-Myc [60], Hif-1α [61], and NFκB [62] are directly regulated by acetylation. Furthermore, metabolic enzymes such as acetyl-CoA synthetase [63] and glycelaldehyde-3-phosphate dehydrogenase (GAPDH), an important glycolytic enzyme [64] are also acetylated.

This study focuses on characterizing the dynamic acetylation/deacetylation of histone H3-K moieties in response to control-normoxia, 5 h anoxia, and 20 h anoxia exposure in the liver of *T.s. elegans*. In particular, protein levels of histone H3, and acetylation levels of three transcriptionally active K residues (H3K14, H3K18, and H3K56) were measured. Protein levels of acetyltransferases 1 (HAT1), general control of amino acid synthesis yeast homolog-like protein 2 (GCN5L2), and p300/CBP-associated factor (PCAF) that are part of the GCN-family of HATs, along with Tip60, a member of the MYST family, and CREB-binding proteins (CBP), that is part of the CPB-p300 HATs were measured. In addition, to elucidate the interplay between acetylation and deacetylation, protein levels of class III nuclear SIRTs, Sirtuin1 (SIRT1), Sirtuin6 (SIRT6), and Sirtuin7 (SIRT7) were measured. Moreover, global and nuclear enzymatic activity of HATs along with enzymatic activity of all nuclear SIRTs was measured. The specific histone H3-K moieties, the respective HATs, and SIRTs were chosen based on their well characterized roles in regulating transcription in the liver as well as their physiological relevance to anaerobiosis. The results suggest a unique regulatory role for histone H3 acetylation in the global suppression of gene expression during anaerobiosis in the freshwater turtle.

Materials and methods

Animal care and treatment

Adult female red-eared sliders ($n = 12$), seven to nine years of age, were purchased from local distributors in Ottawa, ON, Canada. Upon arrival at Carleton University, the turtles were housed in large, aerated tanks filled with dechlorinated tap water (pH = 7) at 11 ± 1 °C and subsequently allowed to acclimate to 4 ± 1 °C for a full week before experiments began. Four control turtles were randomly sampled from this condition. The remaining turtles were transferred to large tubs filled with water that had previously been bubbled with nitrogen gas for 1 h at 5 ± 1 °C. Approximately 2 turtles were added per tub and the water was bubbled with nitrogen gas for 1 h after the last turtle was added to remove all dissolved oxygen. A wire mesh was placed about 5 cm from the water surface to prevent breaching. Post 5 h anoxia submergence, four turtles were randomly sampled. The remaining four turtles were kept in the tubs for 20 h and sacrificed. These turtles were used as the 20 h anoxia experimental condition. Note: All turtles used in this experiment survived the 5 h and 20 h anoxia treatments and red-eared sliders can tolerate and recover from up to three months of absolute anoxia at 4 °C in experimental settings and in iced locked ponds in the wild [1, 2, 5, 7, 12, 20, 65, 66]. The red-eared sliders were euthanized and tissues were excised and immediately placed in liquid nitrogen to stop all cellular processes. The samples were subsequently stored at − 80 °C for later use.

All animals were cared for in accordance to the guidelines of the Canadian Council on Animal Care based on the prior approval of Carleton University Animal Care Committee (protocol #: 13683).

Total soluble protein isolations

500 mg of frozen liver from control, 5 h anoxia, and 20 h anoxia were homogenized using a Polytron homogenizer on high speed for 15 s in 1:2.5 (w:v) homogenization buffer (20 mM HEPES pH 7.5, 200 mM NaCl, 0.1 mM EDTA, 10 mM NaF, 1 mM Na_3VO_4, 10 mM β-glycerophosphate) with 10 µL/mL of protease inhibitor cocktail (Bioshop; Catalog #. PIC001) and a few crystals of phenylmethylsulfonyl fluoride (PMSF). Samples were immediately placed on ice for 5–10 min, vortexed, and centrifuged at 10,000 rpm at 4 °C. Supernatant containing total soluble protein was collected and concentration was determined using the Bradford protein assay (Biorad; Catalog #. 500–0006) with a BSA standard. Liver control, 5 h anoxia, and 20 h anoxia samples were normalized to 10 µg/µL and 50 µL aliquots were reserved for HAT total enzymatic assay. The remaining sample volume was mixed 1:1 (v:v) with 2X-SDS loading buffer (100 mM tris base, 4% (w:v) SDS, 20% (v:v) glycerol, 0.2% (w:v) bromophenol blue, 10% (v:v) 2-mercaptoethanol) to a final concentration of 5 µg/µL. Finally, the samples were boiled for 10 min in a water bath and stored at − 40 °C for later use.

Western immunoblotting

8–10% SDS–polyacrylamide gels were used for HATs and SIRTs quantification, according to the molecular weight of the target protein. The gels were resolved using a Mini-Protean 3 electrophoresis module (Biorad; Catalog #. 164-3301) for 45–90 min at 180 V in 1× tris–glycine running buffer (75.5 g of tris base, 460 g of glycine, 25 g of SDS, and ddH_2O to add up to 2.5 L final volume).

15% tris-tricine gels (30% acrylamide, glycerol, TEMED, 10% APS, and ddH_20) were used for histone H3-total and H3-K modifications and resolved for 180 min at 4 °C using an inner chamber tris/tricine/SDS running buffer (121.1 g of tris base, 179.2 g of tricine, 10 g of SDS in 800 mL of ddH_2O, pH 8.3) and an outer chamber, anode buffer (242 g of tris base in 700 mL of ddH_2O, pH 8.8).

5 µL of Pink Plus Prestained Protein Ladder (Froggabio; Catalog #. PM005-0500K) and 25 µg of a mammalian positive control (*Ictidomys tridecemlineatus* liver) were run alongside each gel as molecular weight references. Linear range of chemiluminescence for all targets were determined based on results obtained from standard curve testing (10–40 µg range)/protein target. Based on the results, 25 µg of total soluble protein was used to quantify H3-total, three H3-K moieties, as well as all HATs. 30 µg of total soluble protein was used to quantify the nuclear SIRTs.

Samples were electroblotted on to 0.25 µm (H3-K modifications) or 0.45 µm (HATs and SIRT) PVDF membranes (Millipore; Catalog #. ISEQ00010 and IPVH00010) in transfer buffer (60.6 g tris base, 288 g glycine, 4 L methanol, 16 L ddH_2O) at 160 mV for 120 min for HATs and SIRTs and 45 min for histone H3-K modifications at RT (room temperature) using Mini-Protean transfer cell (Bio-Rad; Catalog #. 1658004). The PVDF membranes were washed with TBST (10 mM tri-base, 15 mM NaCl, 0.05% (v:v) Tween-20, pH 7.5) and blocked with 2.5–5% milk for 30 min or 1 mg/mL of high molecular weight polyvinyl alcohol (70–100 kDa) for 2 min. After blocking, membranes were re-washed and incubated with primary antibody (diluted 1:1000 (v:v) in TBST) overnight at 4 °C. After incubation, membranes were washed in TBST and incubated with HRP-conjugated anti-rabbit IgG secondary antibody (Bioshop; Catalog #. APA007P) diluted 1:8000 (v:v) in TBST for 40 min at RT. Target protein bands were visualized using enhanced chemiluminescence (ECL) and hydrogen peroxide and a ChemiGenius Bio-Imaging system (Syngene, Frederick, MD). Potential discrepancies in protein loading was corrected for by staining the membranes with coomassie blue protein stain (0.25% (w:v) coomassie blue stain, 7.5% acetic acid, 50% (v:v) methanol) for 15 min and destained with destain solution (25% (v:v) methanol and ddH_2O) for 5 min at RT. Both ECL and coomassie membranes were quantified using GeneTools software (Syngene, Frederick, MD).

Antibodies used in this analysis include, Histone H3-total (Cell Signaling; Catalog #. 4499), H3-K14ac (Cell Signaling; Catalog #. 7627), H3-K18ac (Cell Signaling; Catalog #. 13998), H3-K56ac (Cell Signaling; Catalog #. 4243), HAT1 (Genetex; Catalog #. GTX110643), GCN5L2 (Cell Signaling; Catalog #. 3305), PCAF (Cell Signaling; Catalog #. 3378), Tip60 (Cell Signaling; Catalog #. 12058), CBP (Cell Signaling; Catalog #. 7389), SIRT1 (Active Motif; Catalog #. 39354), SIRT6 (Active Motif; Catalog #. 39912), and SIRT7 (Genetex; Catalog #. GTX54695).

Cytoplasmic and nuclear protein isolations

50 mg of frozen liver was homogenized 1:5 (w:v) in pre-chilled cytoplasmic extraction buffer (100 mM HEPES, 100 mM KCl, 100 mM EDTA, 200 mM β-glycerolphosphate pH 7.9, 10 µL/mL 100 mM DTT, and 10 µL/mL of protease inhibitor cocktail (Bioshop; Catalog # PIC001)) using a mortar and pestle with 3–4 gentle piston strokes. After homogenization, samples were incubated on ice for 30 min with intermittent vortexing. The samples were subsequently centrifuged at 12,000 rpm for 15 min at 4 °C. The supernatant was removed and labeled as the cytoplasmic fraction and the pellet containing the intact nuclei was lysed with nuclear extraction buffer (100 mM HEPES, 2 M NaCl, 5 mM EDTA, 50% (v:v) glycerol, 100 mM β-glycerol phosphate pH 7.9, 10 µL/mL of 100 mM DTT, and 10 µL/mL of protease inhibitor cocktail (Bioshop; Catalog # PIC001)) 1:5 (w:v). After homogenization, samples were sonicated

on high for 10 s and incubated on ice for 10 min to mediate nuclear lysis. The samples were then centrifuged at 14,000 rpms for 10 min at 4 °C and the supernatant was removed and kept as the nuclear fraction. The soluble protein content of the cytoplasmic and nuclear fractions was measured using the Bradford protein assay (Biorad; Catalog #. 500-0006) with a BSA standard. Both cytoplasmic and nuclear fractions were normalized to a final concentration of 5 µg/µL.

To test for the integrity of cytoplasmic and nuclear isolations, 30 µL aliquots of each sample was combined with 2× SDS loading buffer to a final concentration of 2.5 µg/µL and run on a 15% tris–tricine gel and probed with histone H3 diluted 1:1000 (v:v) in TBST. Histone H3 is a nuclear protein and as such would provide insight into the quality of the cytoplasmic and nuclear isolations.

HAT enzymatic activity assay

Global and nuclear-specific enzymatic activity of HATs was measured using the EpiQuik HAT Activity/Inhibition Assay kit from Epigentek (Catalog #. P-4003-96) according to the manufacturer's instructions. Briefly, the assays were conducted using total liver soluble protein extracts and liver nuclear protein extracts in independent wells because HATs are known to acetylate both histones as well as non-histone proteins. We were interested to see whether the overall HAT enzymatic assay profile may differ between total soluble proteins and nuclear protein fractions. A seven-point standard curve ranging from 0.1 ng to 10 ng of HAT assay standard (20 µg/mL; supplied with kit) was used. To determine the linear range of TSE-liver protein that is needed for the assay, a dilution curve ranging from 5 µg to 30 µg of total soluble protein as well as a dilution curve ranging from 5 µg to 30 µg of nuclear protein was tested. Based on the values obtained from the dilution test curves and the standard curves, 10 µg of total soluble protein and 10 µg of nuclear protein was used for the quantification runs. Blank wells consisting of all components of the assay with the exception of protein extracts, were used per assay run. All absorbance readings were measured at 450 nm using a PowerWave HT spectrophotometer (BioTek).

The total HAT activity was calculated using the following formula;

$$\text{HAT Activity}\left(\frac{\text{ng}}{\frac{\text{h}}{\text{mg}}}\right) = \left[\frac{\text{OD(untreated sample} - \text{blank)}}{(\text{protein amount}(\mu\text{g})^{*} \times h^{**} \times \text{slope}^{***})}\right] \times 1000$$

where * is the soluble and nuclear extract (µg) added to the test sample wells, ** is the incubation time at 37 °C, *** is the slope of the line of the standard curve created from input amounts ranging from 0.1, 0.2, 0.5, 1.0, 2.0, 5.0, and 10 ng of protein.

SIRT enzymatic activity assay

Enzymatic activity of nuclear SIRTs was assayed using Epigenase Universal SIRT Activity/Inhibition Fluorometric Assay (Epigentek; Catalog #. P-4037-96). Only the nuclear samples from liver of control, 5 h, and 20 h anoxic red-eared sliders were used for this analysis. The assay was conducted according to the manufacturer's instructions. In brief, a standard curve was prepared by using SIRT assay standard (50 µg/mL; supplied with the kit) at concentrations ranging from 0.2 ng/µL to 5.0 ng/µL along with a dilution curve ranging from 5 µg to 30 µg of liver nuclear samples. Blank wells and No NAD control (NNC) wells were used per assay run. Based on the values obtained from the dilution test curves and the standard curves, 20 µg of liver nuclear extracts were used for the quantification runs. All wells were read using a fluorescence microplate reader at 530ex/590em nm.

Nuclear SIRT activity was calculated using the following formula;

$$\text{SIRT activity}\left(\frac{\text{RFU}}{\frac{\text{min}}{\text{mg}}}\right) = \left[\frac{(\text{sample RFU} - \text{NNC RFU})}{(\text{protein amount}(\mu\text{g})^{*} \times \text{min}^{**})}\right] \times 1000$$

where * is the liver nuclear protein amount used in the analysis, ** is the incubation time at 37 °C.

The total soluble protein and nuclear samples used in the HAT and SIRT enzymatic activity assays were subjected to multiple rounds of Bradford protein quantification with a BSA standard prior to usage and experienced a maximum of one freeze–thaw cycle.

Statistical analysis

To correct for minor irregularities in protein loading, chemiluminescent data for each immunoblot was divided by the absorption density of the corresponding coomassie-stained protein bands in the same lane, not including the target protein, with constant expression across control, 5 h anoxia, and 20 h anoxia exposures. This method has been shown to be far superior to using one housekeeping or reference gene as a loading control since several proteins with constant expression are used for normalization instead of one protein target [67]. Furthermore, natural model systems that employ MRD

as a survival strategy, including red-eared sliders, have been shown to fully reorganize not only the metabolic output but also gene expression, protein translation, and the activity of most enzymes (including housekeeping/reference proteins) [3, 4, 21, 23, 34, 35, 68]. As such, some of the commonly used reference proteins can be differentially expressed across experimental conditions and tissues, and thereby eliminating their usefulness for western immunoblot normalization. Total protein analysis is an alternative technique that can be used to normalize equivalent protein loading within a gel and is independent of the common pitfalls that are associated with using a single protein loading control as a normalization factor [69–72]. Nevertheless, protein level of histone H3 that is often used as a stable, internal loading control in histone modification studies is visually represented in each figure. Target protein bands were identified by running a standard protein molecular weight ladder and a mammalian positive control sample from *I. tridecemlineatus*.

All numerical data are expressed as mean ± SEM ($n = 4$ independent protein isolations from four different animals per experimental condition). Shapiro–Wilk test was used to test for normality, as the sample size is $n < 30$. Data was found to be normally distributed ($p > 0.05$) and as such, parametric tests were carried out. A one-way analysis of variance (ANOVA) with a Tukey post hoc test ($p \leq 0.05$) was used for all pairwise comparisons. SPSS Statistics software (IBM Corp) and GraphPad Prism Version 7 was used for statistical analysis and figure construction, respectively.

Results

The focus of the study was to explore dynamic changes in histone H3-K acetylation along with protein expression of HATs and nuclear SIRTs that may contribute to liver transcriptional regulation in response to oxygen deprivation in an anoxia-tolerant terrestrial vertebrate, the red-eared sliders. Interestingly, a strong suppression of HATs-mediated histone H3 acetylation, a sign of active chromatin, and SIRT-mediated histone deacetylation, a sign of repressed chromatin, was evident in the liver of red-eared sliders, that could play an important role in ATP conservation as part of the overall reduction in metabolic rate during prolonged oxygen deprivation.

H3-K14 acetylation significantly decreased during 5 h anoxia ($F_{(2,11)} = 7.994$, $p = 0.012$; Tukey post hoc, $p = 0.023$) and remained decreased during 20 h anoxia (Tukey post hoc, $p = 0.021$), when compared to the normoxia-control. On the other hand, H3-K18 acetylation increased during 5 h anoxia ($F_{(2,9)} = 19.798$, $p = 0.001$; Tukey post hoc, $p = 0.002$) and returned to control levels during 20 h anoxia (Tukey post hoc, $p = 0.003$). H3-K18 acetylation levels remained unchanged between the control and 20 h anoxia (Tukey post hoc, $p = 0.663$). H3-K56 acetylation ($F_{(2,8)} = 1.042$, $p = 0.409$) and protein levels of H3-total ($F_{(2,11)} = 1.860$, $p = 0.211$) remained unchanged in response to 5 h and 20 h anoxia (Fig. 1a, b).

Protein levels of the corresponding histone H3 acetyltransferases belonging to GCN-family of proteins were also measured (Fig. 2a, b). A robust decrease in HAT1 was evident at 20 h anoxia when compared to the control ($F_{(2,9)} = 12.080$, $p = 0.005$; Tukey post hoc, $p = 0.004$) and 5 h anoxia (Tukey post hoc, $p = 0.046$), yet remained unchanged between the control and 5 h time-point (Tukey post hoc, $p = 0.133$). However, the protein levels of two other prominent GCN-family of acetyltransferases, GCN5L2 ($F_{(2,11)} = 2.487$, $p = 0.138$) and PCAF ($F_{(2,11)} = 0.815$, $p = 0.473$), remained unchanged across all time points.

Tip60, a prominent member of the MYST family of acetyltransferases, significantly decreased during 5 h anoxia

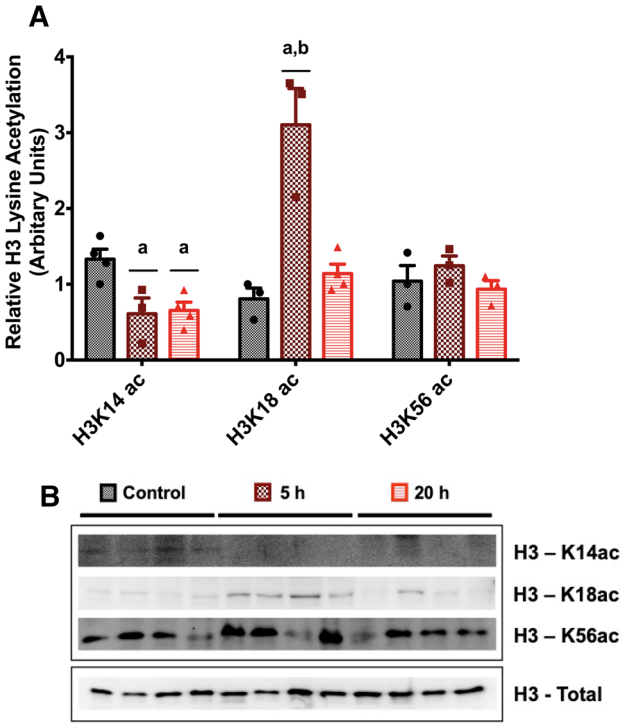

Fig. 1 Histone H3 lysine (K) acetylation in the liver of *T.s. elegans*. **a** Relative levels of H3-K14ac, H3-K18ac, and H3-K56ac levels during control, 5 h anoxia, and 20 h anoxia as determined by western immunoblotting. **b** Immunoblot band image of the targets. H3-total is presented as a stable, internal loading control. Immunoblot band intensities were normalized against the summed intensity of coomassie-stained protein bands in the same lane (without including the target protein)/immunoblot. Data are mean ± SEM ($n = 4$/experimental condition of independent protein isolations from different animals). The same $n = 4$ control, $n = 4$, 5 h anoxic, and $n = 4$, 20 h anoxic turtles were used in each immunoblot. **a** represents statistically significant differences from the control ($p \leq 0.05$), **b** represents statistically significant differences from 5 h anoxia value as determined by one-way ANOVA with a Tukey post hoc test ($p \leq 0.05$)

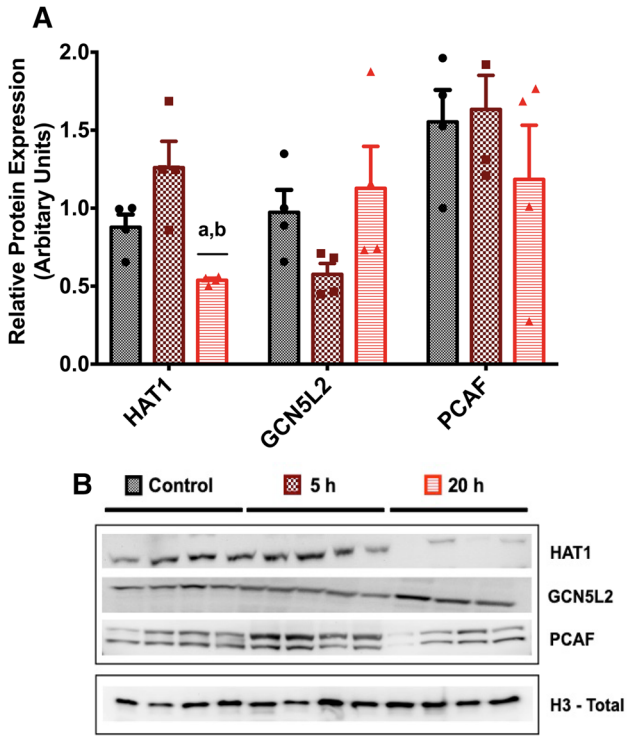

Fig. 2 Protein levels of GCN-family of acetyltransferases in the liver of *T.s. elegans*. **a** Relative protein levels of HAT1, GCN5L2, and PCAF during control, 5 h, and 20 h anoxia as determined by western immunoblotting. **b** Immunoblot band images of the targets. Other information as in Fig. 1

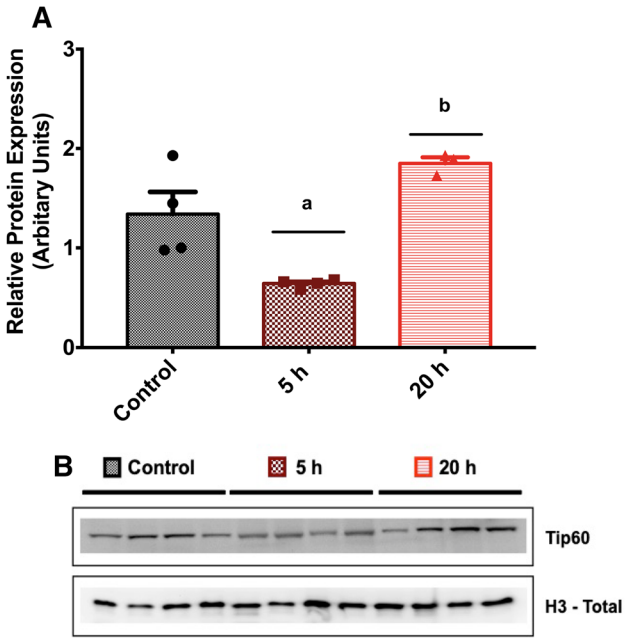

Fig. 3 Protein levels of MYST family of acetyltransferases in the liver of *T.s. elegans*. **a** Relative protein level of Tip60 during control, 5 h, and 20 h anoxia as determined by western immunoblotting. **b** Immunoblot band image of the target. Other information as in Fig. 1

when compared to the normoxia-control ($F_{(2,10)} = 16.348$, $p = 0.001$; Tukey post hoc, $p = 0.019$) and returned to control levels during 20 h anoxia (Tukey post hoc, $p = 0.001$). Tip60 protein level between the control and 20 h anoxia remained unchanged (Tukey post hoc, $p = 0.101$; Fig. 3a, b).

CBP protein, a vital component of CBP-p300 HATs, robustly decreased during 5 h anoxia ($F_{(2,10)} = 38.847$, $p < 0.0001$; Tukey post hoc, $p < 0.0001$) and 20 h anoxia (Tukey post hoc, $p = 0.0001$) when compared to the control. CBP protein level between 5 and 20 h anoxia remained unchanged (Tukey post hoc, $p = 0.275$; Fig. 4a, b).

Global enzymatic activity of HATs remained unchanged in response to 5 h and 20 h anoxia when compared to the control ($F_{(2,11)} = 0.013$, $p = 0.987$). However, HAT enzymatic activity of the nuclear protein fraction significantly decreased in response to 5 h ($F_{(2,11)} = 55.560$, $p < 0.001$; Tukey post hoc, $p < 0.0001$) and 20 h anoxia (Tukey post hoc, $p < 0.0001$), when compared to the control. Nuclear HAT activity remained unchanged between 5 and 20 h anoxia (Tukey post hoc, $p = 0.411$; Fig. 5).

Protein levels of class III HDACs, the nuclear SIRTs, varied across 5 h and 20 h anoxia, when compared to the control (Fig. 6a, b). In particular, SIRT1 levels significantly decreased during 20 h anoxia when compared to the control

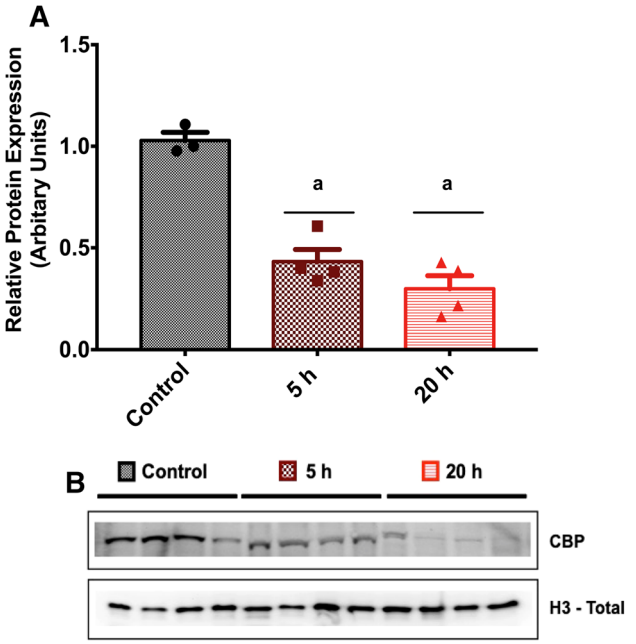

Fig. 4 Protein levels of CBP/p300 family of acetyltransferases in the liver of *T.s. elegans*. **a** Relative protein level of CBP during control, 5 h, and 20 h anoxia as determined by western immunoblotting. **b** Immunoblot band image of the target. Other information as in Fig. 1

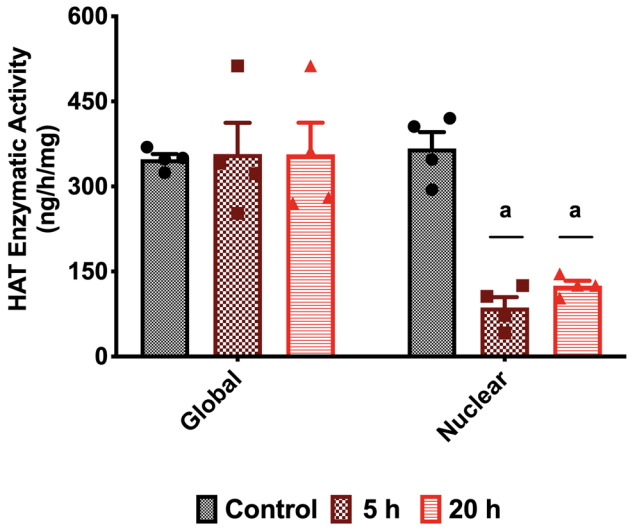

Fig. 5 Enzymatic activity of histone acetyltransferases (HATs) in the liver of *T.s. elegans*. Global HAT enzymatic activity (ng/h/mg) as well as nuclear HAT enzymatic activity (ng/h/mg) during control, 5 h anoxia, and 20 h anoxia as determined by EpiQuik HAT Activity/Inhibition Colorimetric Assay kit from Epigentek. Data are mean ± SEM ($n = 4$/experimental condition of independent protein isolations from different animals). **a** represents statistically significant differences from the control ($p \leq 0.05$), **b** represents statistically significant differences from 5 h anoxia value as determined by one-way ANOVA with a Tukey post hoc test ($p \leq 0.05$)

($F_{(2,11)} = 67.861$, $p < 0.0001$; Tukey post hoc, $p < 0.0001$) and 5 h anoxia (Tukey post hoc, $p < 0.0001$), yet remained unchanged between the control and 5 h anoxia (Tukey post hoc, $p = 0.284$). Moreover, SIRT6 significantly decreased in response to 5 h anoxia ($F_{(2,11)} = 10.318$, $p < 0.005$; Tukey post hoc, $p = 0.036$) and 20 h anoxia (Tukey post hoc, $p = 0.004$), when compared to the control. There were limited changes in SIRT6 protein levels between 5 and 20 h anoxia (Tukey post hoc, $p = 0.361$). SIRT7 protein levels remained unchanged in response to 5 h and 20 h anoxia ($F_{(2,10)} = 2.952$, $p = 0.110$).

Enzymatic activity of nuclear SIRTs significantly decreased in response to 5 h ($F_{(2,11)} = 22.074$, $p < 0.001$; Tukey post hoc, $p < 0.0001$) and 20 h anoxia (Tukey post hoc, $p = 0.001$), when compared to the control. Nuclear SIRT activity remained unchanged between 5 and 20 h anoxia (Tukey post hoc, $p = 0.773$; Fig. 6c).

Discussion

Present study explored transcriptional regulation, a unique characteristic of MRD, in the context of histone H3-K acetylation and deacetylation in the liver during control, 5 h anoxia, and 20 h anoxia in red-eared sliders. Liver was exclusively chosen for this study because liver is the primary site of glycogen storage and glycogenolysis in anoxia-tolerant freshwater turtles [2, 13, 35, 68]. Glycogen is the sole metabolic fuel that can be broken down to produce ATP during anaerobiosis. Furthermore, anoxic hepatocytes have been reported to decrease the overall metabolic rate by 90% during long-term oxygen deprivation [73], yet liver continues to be proliferative, active, and demonstrate target-specific increases in gene expression during MRD. As such, liver is an important organ to investigate to understand the intricate balance between a global suppression and target-specific increases in gene expression, a key characteristic of MRD. Moreover, several epigenetic modifiers including DNMTs (DNA methyltransferases) [71], HKMTs (histone lysine methyltransferases) [70], non-NAD^+-dependent HDACs [72], and miRNAs [31, 33] were elucidated as prominent players of transcriptional regulation in the liver of red-eared sliders during 5 h and 20 h anoxia by previous studies. As such, liver is an optimal tissue that can be used to investigate an additional layer of transcriptional regulation during anaerobiosis; the balance between transcriptionally permissive histone H3-K acetylation via HATs and transcriptionally repressive histone H3-K deacetylation via SIRTs. Further, this study is a continuation of an earlier study by Krivoruchko and Storey, where the role of non-NAD^+ dependent HDACs, belonging to class I, II, and IV, was investigated in anerobic red-eared sliders [72]. Interestingly, they reported a significant increase in HDAC mRNA and protein levels along with a decrease in acetylation at targeted H3-K moieties during 5 h and 20 h anoxia in the liver. Overall, they identified class I, II, and IV HDACs to play a key role in global transcriptional repression during MRD, however due to the lack of well-tested antibodies and enzymatic activity assays that were commercially available at the time, Krivoruchko and Storey did not explore the role of NAD^+ dependent class III HDACs. As such, in this study, we have focused on uncovering the interplay between class III HDACs (transcriptional repressors) and HATs (transcriptional activators) and explored their role in regulating histone H3 acetylation during MRD.

Histone H3 (total) protein levels remained unchanged in response to anoxia (Fig. 1a, b). A stable maintenance of histone H3 protein levels is expected, as post-translational modifications (PTMs) are more swift and energy-wise methods of controlling protein function, activity, cellular distribution, and protein–protein interactions during MRD [4, 21, 35, 68]. Histone H3 was also used as a stable, internal reference control to demonstrate 1) the changes in acetylation of K moieties during anoxia are not due to changes in histone H3 protein levels, but rather can be attributed to epigenetic modifications, and 2) minimal variability exist in protein loading across western immunoblots used in the study. Furthermore, these results correspond to the earlier findings of Krivoruchko and Storey, in which histone H3

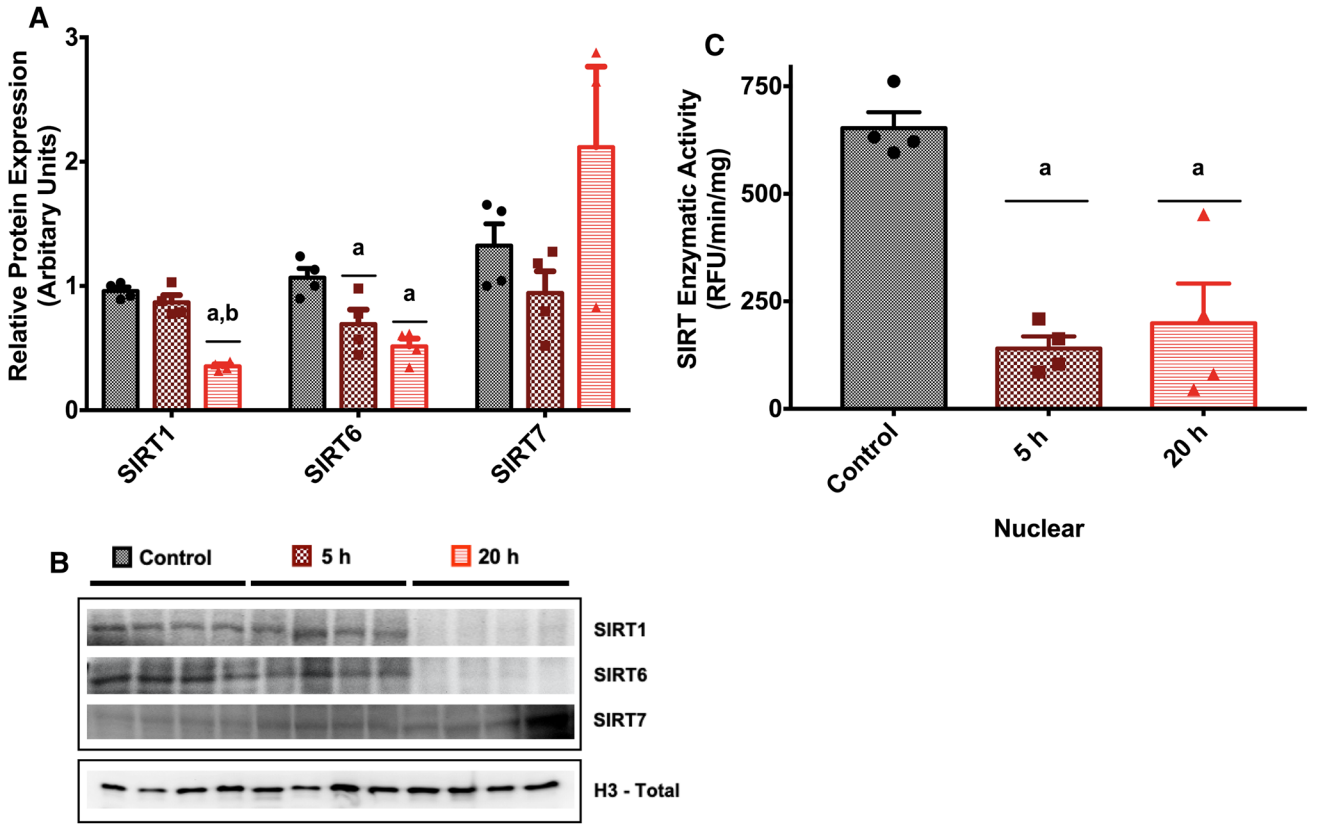

Fig. 6 Histone H3 lysine (K) deacetylation in the liver of *T.s. elegans*. *a* Relative protein expression levels of three nuclear, class III histone deacetylases, sirtuins (SIRTs), SIRT1, SIRT6, and SIRT7, during control, 5 h, and 20 h anoxia as determined by western immunoblotting. **b** Immunoblot band images of the targets. **c** Enzymatic activity (RFU/min/mg) of nuclear SIRTs during control, 5 h anoxia, and 20 h anoxia as determined by Epigenase Universal SIRT Activity/Inhibition Fluorometric Assay. Data are mean ± SEM ($n = 4$/experimental condition of independent protein isolations from different animals). **a** represents statistically significant differences from the control ($p \leq 0.05$), **b** represents statistically significant differences from 5 h anoxia value as determined by one-way ANOVA with a Tukey post hoc test ($p \leq 0.05$)

protein levels remained unchanged in response to anoxia in red-earlier sliders [72].

H3-K14ac, an epigenetic modification that is typically associated with active promoters, significantly decreased during 5 h and 20 h anoxia (Fig. 1a, b). Interestingly, genome-wide distribution of H3-K14ac and H3-K9ac levels were found to be highly correlated and typically located in euchromatic-active promoter regions, gene regulatory elements, as well as bivalent promoters [74]. Correspondingly, H3-K9ac levels also decreased in response to anoxia in the liver of red-eared sliders [72]. As such, significant decreases in H3-K14ac and H3-K9ac levels may indicate a potential increase in chromatin condensation and a state of transcriptional repression in the liver during short and long-term oxygen deprivation. On the contrary, H3-K18ac levels, an additional acetylation moiety that promote open-chromatin, significantly increased during 5 h anoxia and returned back to control levels during 20 h anoxia (Fig. 1a, b). However, the increase in H3-K18ac reported herein may not necessarily indicate a global increase in transcription during a low energy state, where the overall transcriptional output is lower, but rather an increase in H3-K18ac could represent target-specific enhancement of candidate genes; another key characteristic of MRD. For example, NFκB is a master transcription factor that is central to the anoxia stress response and a plausible correlation between NFκB expression and increased H3-K18ac levels in the promoter regions have previously been reported [75]. Correspondingly, NFκB pathway is shown to be active during anoxia in the liver of red-eared sliders and play an important role in regulating protective, anti-oxidation responses [17]. As such, it would be interesting to map site-specific H3-K18ac patterns in the regulatory regions of NFκB promoter through chromatin immunoprecipitation sequencing (ChIP-Seq.) technology in a future study. Lastly, global H3-K56ac levels remained unchanged in response to 5 h and 20 h anoxia in the liver (Fig. 1a, b). H3-K56ac levels are potentially maintained throughout short and long-term anoxia in the red-eared sliders because H3-K56ac modifications

are highly enriched at the sites of DNA repair [76]. As such, H3-K56ac may play a prominent role in DNA damage response, a key protective mechanism employed by freshwater turtles to combat against large influx of reactive oxygen species during bouts of anaerobiosis. Indeed, a recent liver transcriptomics study on freshwater turtles by Biggar et al. identified DNA damage repair as one of the top Kyoto Encyclopedia of Genes and Genomes (KEGG) pathways that were enriched with differentially expressed genes during 5 h and 20 h anoxia [77]. As such, future work is needed to explore the link between DNA damage repair and the relevant histone moieties, writers, and erasers during anaerobiosis in freshwater turtles.

HATs are a diverse group of enzymes that are categorized based on the catalytic domains and the specificity of the K residues they acetylate [78]. GNATs including HAT1, GCN5L2, and PCAF along with Hpa2 and Nut1a catalyze the transfer of acetyl groups from acetyl-CoA to a primary amine [45, 46, 75, 79]. GNATs are well-established epigenetic players that induce post-translational modifications on metabolic enzymes, transcription factors, as well as histones, Histone H3 acetylation in particular is associated with active transcription and euchromatic open-chromatin [45, 48, 80–82]. HAT1 protein levels significantly decreased during 20 h anoxia when compared to the control and 5 h anoxia (Fig. 2a, b). HAT1 directly regulates H3-K14 acetylation and thus the decrease in HAT1 protein level along with the robust decrease in H3-K14ac reported herein, may indicate an overall decrease in histone acetylation in red-eared sliders as a way of limiting the overall transcriptional output during long-term anoxia in the liver. On the contrary, protein levels of two other established GNATs, GCN5L2 and PCAF, remained unchanged during 5 h and 20 h anoxia (Fig. 2a, b). GCN5L2 is an activator of transcription initiation and is recruited to gene promoters [45, 46]. GCN5L2 also acetylate H3-K14 and H3-K23 residues [83, 84]. However, H3-K14 (Fig. 1a, b) and H3-K23 [72] decreased in response to anoxia in red-eared sliders. Therefore, although protein levels of GCN5L2 remained unchanged in response to anoxia, the GCN5L2 enzymatic activity may have been affected by post-translational modifications (PTMs). Indeed, GCN5L2 activity is regulated by reversible protein phosphorylation (RPP) by DNA-dependent protein kinase (DNA-PK) [85]. Similar to GCN5L2 levels, PCAF protein levels also remained unchanged in response to anoxia in red-reared sliders (Fig. 1a, b). PCAF has been reported to acetylate and reduce the overall enzymatic activity of pyruvate kinase (PK), one of the major enzymes that control the glycolytic flux [86]. Correspondingly, turtles use covalent modifications to regulate enzymatic activity of PK, as part of an anoxia-tolerant metabolic strategy [23]. Therefore, PCAF protein expression may remain stagnant during anoxia in the liver as a means of regulating the glycolytic flux. Post-translational regulation of non-histone proteins by GNAT-family of acetyltransferases requires further investigation.

The MYST family of acetyltransferases include Morf, MOZ, Ybf2, Sas2, and Tip60. Possible functions of the Tip60 complex include transcriptional activation as well as DNA repair [79]. MYST family of HATs acetylate six K residues of histone proteins including H2A-K5, H3-K14, and H4-K5/8/12/16 [87]. Moreover, Tip60 was exclusively chosen to represent the MYST family of HATs in this study due to their vital role in regulating histone and non-histone protein function during anaerobiosis. Tip60 is a conserved coactivator of HIF-1α, a critical modulator of anaerobiosis and the cellular response to hypoxia in vertebrates [36]. In particular, HIF-1α interacts with and recruits Tip60 to open-chromatin and a majority of HIF-1α regulated genes require Tip60 coactivation for expression [61]. HIF-1α is the central transcription factor of the hypoxia response in freshwater turtles and other anaerobic vertebrates, where low oxygen levels activate HIF-1α and that in turn upregulates the expression of variety of downstream genes, including VEGF and erythropoietin, that help improve oxygen delivery to vital organs, glycolytic enzymes, including PDK that increase the overall glycolytic flux, and glucose transporters, including GLUT4 [3, 4, 21]. Correspondingly, HIF-1α protein levels and nuclear localization were shown to increase in response to 5 h anoxia in *T. scripta elegans* [36]. Moreover, Tip60 is a vital post-translational modifier of another central transcription factor, p53. In particular, Tip60-dependent acetylation of p53 at K120 residue has been shown to modulate the cellular functions of p53, where the decision between promoting cell cycle arrest and/or apoptosis is determined based on the presence of the K120 acetyl residue [88]. Interestingly, tissue-specific regulation of p53 was observed in response to anoxia in *T. scripta elegans*, where the liver exhibited the largest increase in p53 expression and activation via post-translational modifications of select serine and lysine residues [27]. Further, Zhang et al. also reported increased expression of genes that are directly regulated by p53, including 14-3-3α, GADD45α, and Pgm. Taken together, they concluded that p53 and its associated co-activators (kinases and acetyltransferases) may play a vital role in regulating MRD during anaerobiosis in freshwater turtles. Tip60 protein levels decreased in response to 5 h anoxia and returned back to control levels during 20 h anoxia (Fig. 3a, b) and similarly H3-K14ac levels decreased in response to anoxia (Fig. 1a, b). As such, the decrease in Tip60 levels during 5 h anoxia could be a tissue-specific response to anaerobiosis that aid freshwater turtles in modulating the global transcriptional response as well as target-specific non-histone protein function.

CBP is not only a well-established HAT that directly targets H3-K56 moieties but it is also a well-established co-transcriptional regulator of p53 at K373 residue [87].

CBP protein levels decreased during 5 h and 20 h anoxia (Fig. 4a, b). Although H3-K56ac levels remained unchanged in response to anoxia (Fig. 1a, b), p53-K373ac levels significantly decreased in response to 5 h and 20 h anoxia in the liver of red-eared sliders [27]. p53 is a transcription factor that has major roles in regulating cell cycle, apoptosis, DNA damage repair, as well as energy metabolism [89–92] and p53-K373ac blocks ubiquitination of this lysine site and lead to enhanced activation and survival of p53 [27]. Therefore, similar to the decrease in Tip60 protein level, the decrease in CBP that is seen during 5 h and 20 h anoxia herein (Fig. 4a, b) could contribute to target-specific regulation of non-histone proteins that are necessary for anoxia tolerance and survival in red-eared sliders.

Global as well as nuclear HAT enzymatic activity yielded very interesting results. Although, the global enzymatic activity of all HATs that can acetylate K residues of both histone and non-histone proteins remained unchanged during 5 h and 20 h anoxia, nuclear HATs that primarily acetylate histone proteins decreased in activity during anoxia (Fig. 5). These results further corroborate the overall decrease in histone H3 acetylation and an overall decrease in HAT1, Tip60, and CBP protein levels seen in the study. As such, the suppression of histone H3-K acetylation during anoxia in red-eared sliders could be a prominent characteristic of anaerobiosis and MRD.

SIRTs are NAD^+-dependent class III HDACs, that regulate a variety of cellular processes including histone deacetylation, DNA repair, metabolism, glucose homeostasis, as well as aging [69, 93, 94]. In the context of turtle anaerobiosis, class I and II HDACs were shown to increase in mRNA and protein levels during 5 h and 20 h anoxia and was postulated to be a major characteristic of anoxia survival [72]. However, the potential involvement of nuclear SIRTs (SIRT1, SIRT6, and SIRT7) in anaerobiosis required further exploration. Overall, the results suggest limited nuclear SIRT regulation in the liver during 5 h and 20 h anoxia in red-eared sliders (Fig. 6a, b). In particular, protein levels of SIRT1 and SIRT6 decreased in response to anoxia, whereas SIRT7 protein levels remained unchanged. Correspondingly, overall enzymatic activity of nuclear SIRTs significantly decreased during 5 h and 20 h anoxia (Fig. 6c). A decrease in nuclear SIRT protein and enzymatic activity during prolonged oxygen deprivation could be part of the global suppression in gene expression during MRD that has been reported previously in red-eared sliders. MRD is the combinatorial suppression of most energy consuming processes and reprioritization of ATP towards cellular processes that are necessary for anoxia survival [3, 4, 21]. Therefore, during MRD, hepatocytes could be monopolizing class I and II HDACs to drive histone H3 deacetylation and enforce a state of chromatin condensation in *T.s. elegans* [72], while limiting the protein levels and enzymatic activity of nuclear SIRTs. Dependence on one group of proteins and/or enzymes while temporarily shutting down the expression and/or activity of another group of functionally similar proteins is a common characteristic of MRD [3, 4, 21, 68]. Further, SIRT enzymatic activity primarily depends on the availability of NAD^+ [69], yet a drastic decrease in NAD^+/NADH pools have been reported in the cytoplasm and mitochondrial compartment of hepatocytes in response to short and long-term hypoxia in freshwater turtles [95]. In an anaerobic cell, with the absence of oxygen (the final acceptor of electrons in the electron transport chain) oxidative phosphorylation comes to a halt and glycolysis becomes the primary mode of ATP generation. Glycolysis requires NAD^+ to function as an electron acceptor in the conversion of glyceraldehyde 3-phosphate into 1,3-bisphosphoglycerate and NAD^+ levels are replenished through the conversation of pyruvate into lactate. Given all cells contain a limited number of NAD^+ molecules that are cycled back and forth between the oxidized (NAD^+) and reduced (NADH) form, it is imperative to maintain a proper balance between NAD^+/NADH molecules in anaerobic cells [2, 7, 82, 96]. As such, the decrease in SIRT enzymatic activity and the reliance on non-NAD^+-dependent HDACs to modulate protein deacetylation during anaerobiosis, may be an energy conservation mechanism employed by the freshwater turtles to reduce the use of NAD^+ pools.

In summary, this study reports an overall decrease in histone H3-K acetylation across three transcriptionally relevant histone modifications in the liver along with an overall decrease in protein levels and enzymatic activity of HATs and nuclear SIRTs during short and long-term anoxia in red-eared sliders. Maintaining a proper balance between permissive chromatin and repressive chromatin is of utmost importance in a low energy, anoxia state, where anaerobic glycolysis is the sole source of ATP production. Consequently, overall decrease in histone H3-K acetylation reported here could be a notable characteristic of MRD in anoxia-tolerant freshwater turtles.

Author contributions SW: Conceived and designed the experiment, prepared all material, conducted all experiments, data collection, and analysis and wrote the paper. KBS: Provided all reagents and equipment necessary for the project, provided supervision, and assisted with manuscript writing. All authors read and approved the final manuscript.

Funding This work was supported by a Discovery Grant (#6793) awarded to Dr. Kenneth B Storey from the Natural Sciences and Engineering Research Council of Canada (NSERC) and Dr. Kenneth B. Storey holds the Canada Research Chair in Molecular Physiology. Dr. Sanoji Wijenayake holds a NSERC Postdoctoral Research Fellowship at the University of Toronto.

Data availability All raw data will be available upon request by the corresponding author.

Compliance with ethical standards

Conflict of interest Authors declare that they have no conflicts of interest.

Consent to participate Not applicable.

Consent for publication Not applicable.

Ethical approval All animals were cared for in accordance to the guidelines of the Canadian Council on Animal Care based on the prior approval of Carleton University Animal Care Committee (protocol #: 13683).

References

1. Jackson D, Ultsch G (1982) Long-term submergence at 3°C of the turtle, *Chrysemys picta bellii*, in normoxic and severely hypoxic water: II. Extracellular ionic responses to extreme lactic acidosis. J Exp Biol 29–43
2. Jackson D (1968) Metabolic depression and oxygen depletion in the diving turtle. J Appl Physiol 24:503–509
3. Storey K, Storey J (1990) Metabolic rate depression and biochemical adaptation in anaerobiosis, hibernation and estivation. Q Rev Biol 65:145–174. https://doi.org/10.4172/2157-7625.1000224
4. Storey K (2007) Anoxia tolerance in turtles: metabolic regulation and gene expression. Comp Biochem Physiol Part A Mol Integr Physiol 147:263–276. https://doi.org/10.1016/j.cbpa.2006.03.019
5. Hochachka P (1988) Metabolic suppression and oxygen availability. Can J Zool 66:152–158. https://doi.org/10.1139/z88-021
6. Hochachka P (1986) Defense strategies against hypoxia and hypothermia. Science 231:234–241. https://doi.org/10.1126/science.2417316
7. Jackson DC (2000) Living without oxygen: lessons from the freshwater turtle. Comp Biochem Physiol Part A Mol Integr Physiol 125:299–315. https://doi.org/10.1016/S1095-6433(00)00160-4
8. Storey K, Storey J (1992) Natural freeze tolerance in ectothermic vertebrates. Annu Rev Physiol 54:619–637. https://doi.org/10.1146/annurev.ph.54.030192.003155
9. Hermes-Lima M, Zenteno-Savín T (2002) Animal response to drastic changes in oxygen availability and physiological oxidative stress. Comp Biochem Physiol Toxicol Pharmacol 133:537–556. https://doi.org/10.1016/S1532-0456(02)00080-7
10. Jackson D, Taylor S, Asare V et al (2006) Comparative shell buffering properties correlate with anoxia tolerance in freshwater turtles. AJP Regul Integr Comp Physiol 292:R1008–R1015. https://doi.org/10.1152/ajpregu.00519.2006
11. Jackson D (1997) Lactate accumulation in the shell of the turtle, *Chrysemys picta bellii*, during anoxia at 3 and 10°C. J Exp Biol 200:2295–2300
12. Jackson D, Heisler N (1983) Intracellular and extracellular acid–base and electrolyte status of submerged anoxic turtles at 3°C. Respir Physiol 53:187–201
13. Jackson D, Toney V, Okamoto S (1999) Lactate distribution and metabolism during and after anoxia in the turtle, Chrysemys picta bellii. Am J Physiol 271:R409–R416
14. Jackson D, Crocker C, Ultsch G (2000) Bone and shell contribution to lactic acid buffering of submerged turtles *Chrysemys picta bellii* at 3°C. Am J Physiol - Regul Integr Comp Physiol 278:R1564–1571
15. Krivoruchko A, Storey K (2010) Activation of antioxidant defenses in response to freezing in freeze-tolerant painted turtle hatchlings. Biochim Biophys Acta - Gen Subj 1800:662–668. https://doi.org/10.1016/j.bbagen.2010.03.015
16. Krivoruchko A, Storey K (2010) Regulation of the heat shock response under anoxia in the turtle, *Trachemys scripta elegans*. J Comp Physiol B 180:403–414. https://doi.org/10.1007/s00360-009-0414-9
17. Krivoruchko A, Storey K (2010) Molecular mechanisms of turtle anoxia tolerance: a role for NF-κB. Gene 450:63–69. https://doi.org/10.1016/j.gene.2009.10.005
18. Krivoruchko A, Storey K (2013) Activation of the unfolded protein response during anoxia exposure in the turtle *Trachemys scripta elegans*. Mol Cell Biochem 374:91–103. https://doi.org/10.1007/s11010-012-1508-3
19. Willmore W, Storey KB (1997) Antioxidant systems and anoxia tolerance in a freshwater turtle *Trachemys scripta elegans*. Mol Cell Biochem 170:177–185. https://doi.org/10.1023/A:1006817806010
20. Hochachka P, Buck L, Doll C, Land S (1996) Unifying theory of hypoxia tolerance: molecular/metabolic defense and rescue mechanisms for surviving oxygen lack. Proc Natl Acad Sci U S A 93:9493–9498. https://doi.org/10.1073/pnas.93.18.9493
21. Storey K (1996) Metabolic adaptations supporting anoxia tolerance in reptiles: recent advances. Comp Biochem Physiol Part B Comp Biochem 113:23–35. https://doi.org/10.1016/0305-0491(95)02043-8
22. Dawson NJ, Biggar KK, Storey KB (2013) Characterization of fructose-1,6-bisphosphate aldolase during anoxia in the tolerant turtle, *Trachemys scripta elegans*: an assessment of enzyme activity, expression and structure. PLoS ONE 8:e68830. https://doi.org/10.1371/journal.pone.0068830
23. Brooks S, Storey K (1989) Regulation of glycolytic enzymes during anoxia in the turtle *Pseudemys scripta*. Am J Physiol 257:R278–R283. https://doi.org/10.1152/ajpregu.1989.257.2.R278
24. Bell R, Storey K (2012) Regulation of liver glutamate dehydrogenase from an anoxia-tolerant freshwater turtle. HOAJ Biol 1:1–3. https://doi.org/10.7243/2050-0874-1-3
25. Mehrani H, Storey K (1995) Enzymatic control of glycogenolysis during anoxic submergence in the freshwater turtle *Trachemys scripta*. Int J Biochem Cell Biol 821–830:821–830. https://doi.org/10.1016/1357-2725(95)00042-N
26. Dawson N, Bell R, Storey K (2013) Purification and properties of white muscle lactate dehydrogenase from the anoxia-tolerant turtle, the red-eared slider, *Trachemys scripta elegans*. Enzyme Res 2013:1–8. https://doi.org/10.1155/2013/784973
27. Zhang J, Biggar KK, Storey KB (2013) Regulation of p53 by reversible post-transcriptional and post-translational mechanisms in liver and skeletal muscle of an anoxia tolerant turtle, *Trachemys scripta elegans*. Gene 513:147–155. https://doi.org/10.1016/j.gene.2012.10.049
28. Bansal S, Biggar KK, Krivoruchko A, Storey KB (2016) Response of the JAK-STAT signaling pathway to oxygen deprivation in the red eared slider turtle, *Trachemys scripta elegans*. Gene 593:34–40. https://doi.org/10.1016/j.gene.2016.08.010
29. Biggar KK, Storey KB (2012) Evidence for cell cycle suppression and microRNA regulation of cyclin D1 during anoxia exposure in turtles. Cell Cycle 11:1705–1713. https://doi.org/10.4161/cc.19790
30. Krivoruchko A, Storey K (2013) Anoxia-responsive regulation of the FoxO transcription factors in freshwater turtles, *Trachemys scripta elegans*. Biochim Biophys Acta - Gen Subj 1830:4990–4998. https://doi.org/10.1016/j.bbagen.2013.06.034
31. Biggar K, Storey K (2015) Insight into post-transcriptional gene regulation: stress-responsive microRNAs and their role in the environmental stress survival of tolerant animals. J Exp Biol 218:1281–1289. https://doi.org/10.1242/jeb.104828

32. Biggar KK, Kornfeld SF, Storey KB (2011) Amplification and sequencing of mature microRNAs in uncharacterized animal models using stem–loop reverse transcription–polymerase chain reaction
33. Biggar K, Storey K (2011) The emerging roles of microRNAs in the molecular responses of metabolic rate depression. J Mol Cell Biol 3:167–175. https://doi.org/10.1093/jmcb/mjq045
34. Brooks S, Storey K (1993) De novo protein synthesis and protein phosphorylation during anoxia and recovery in the red-eared turtle. Am J Physiol 265:R1380–R1386
35. Storey K, Storey J (2007) Tribute to P. L. Lutz: putting life on 'pause': molecular regulation of hypometabolism. J Exp Biol 210:1700–1714. https://doi.org/10.1242/jeb.02716
36. Biggar K, Groom A, Storey K (2011) Hypometabolism and turtles: Physiological and molecular strategies of anoxic survival. In: Nowakowska A, Caputa M (eds) Hypometabolism: strategies of survival in vertebrates and invertebrates. Research Signpost, Kerala, pp 57–94
37. Choudhary C, Mann M (2010) Decoding signalling networks by mass spectrometry-based proteomics. Nat Rev Mol Cell Biol 11:427–439. https://doi.org/10.1038/nrm2900
38. Strahl B, Allis C (2000) The language of covalent histone modifications. Nature 403:41–45. https://doi.org/10.1038/47412
39. Shahbazian M, Grunstein M (2007) Functions of site-specific histone acetylation and deacetylation. Annu Rev Biochem 76:75–100. https://doi.org/10.1146/annurev.biochem.76.052705.162114
40. Berger S (2002) Histone modifications in transcriptional regulation. Curr Opin Genet Dev 12:142–148. https://doi.org/10.1016/S0959-437X(02)00279-4
41. Clayton A, Hazzalin C, Mahadevan L (2006) Enhanced histone acetylation and transcription: a dynamic perspective. Mol Cell 23:289–296. https://doi.org/10.1016/j.molcel.2006.06.017
42. Struhl K (1998) Histone acetylation and transcriptional regulatory mechanisms. Genes Dev 12:599–606
43. Wade P, Pruss D, Wolffe A (1997) Histone acetylation: chromatin in action. Trends Biochem Sci 22:128–132. https://doi.org/10.1016/S0968-0004(97)01016-5
44. Eberharter A, Becker P (2002) Histone acetylation: a switch between repressive and permissive chromatin: second in review series on chromatin dynamics. EMBO Rep 3:224–229. https://doi.org/10.1093/embo-reports/kvf053
45. Dyda F, Klein D, Hickman A (2000) GCN5-related *N*-acetyltransferases: a structural overview. Annu Rev Biophys Biomol Struct 29:81–103. https://doi.org/10.1146/annurev.biophys.29.1.81
46. Neuwald A, Landsman D (1997) GCN5-related histone N-acetyltransferases belong to a diverse superfamily that includes the yeast SPT10 protein. Trends Biochem Sci 22:154–155
47. Avvakumov N, Cote J (2007) The MYST family of histone acetyltransferases and their intimate links to cancer. Oncogene 26:5395–5407. https://doi.org/10.1038/sj.onc.1210608
48. Sterner D, Berger S (2000) Acetylation of histones and transcription-related factors. Microbiol Mol Biol Rev 64:435–459
49. Bannister A, Kouzarides T (1996) The CBP co-activator is a histone acetyltransferase. Nature 384:641–643. https://doi.org/10.1038/384641a0
50. Liu X, Wang L, Zhao K et al (2008) The structural basis of protein acetylation by the p300/CBP transcriptional coactivator. Nature 451:846–850. https://doi.org/10.1038/nature06546
51. Mizzen C, Yang X, Kokubo T et al (1996) The TAF(II)250 subunit of TFIID has histone acetyltransferase activity. Cell 87:1261–1270
52. O'Malley B, Spencer T, Jenster G et al (1997) Steroid receptor coactivator-1 is a histone acetyltransferase. Nature 389:194–198. https://doi.org/10.1038/38304
53. Kawasaki H, Schiltz L, Chiu R et al (2000) ATF-2 has intrinsic histone acetyltransferase activity which is modulated by phosphorylation. Nature 405:195–200. https://doi.org/10.1038/35012097
54. Delcuve G, Khan D, Davie J et al (2012) Roles of histone deacetylases in epigenetic regulation: emerging paradigms from studies with inhibitors. Clin Epigenetics 4:5. https://doi.org/10.1186/1868-7083-4-5
55. Polevoda B, Sherman F (2000) Nalpha -terminal acetylation of eukaryotic proteins. J Biol Chem 275:36479–36482. https://doi.org/10.1074/jbc.R000023200
56. Glozak M, Sengupta N, Zhang X, Seto E (2005) Acetylation and deacetylation of non-histone proteins. Gene 363:15–23. https://doi.org/10.1016/j.gene.2005.09.010
57. Gu W, Roeder R (1997) Activation of p53 sequence-specific DNA binding by acetylation of the p53 C-terminal domain. Cell 90:595–606. https://doi.org/10.1016/s0092-8674(00)80521-8
58. Munshi N, Merika M, Yie J et al (1998) Acetylation of HMG I(Y) by CBP turns off IFN? Expression by disrupting the enhanceosome. Mol Cell 2:457–467. https://doi.org/10.1016/S1097-2765(00)80145-8
59. Wang R, Cherukuri P, Luo J (2005) Activation of Stat3 sequence-specific DNA binding and transcription by p300/CREB-binding protein-mediated acetylation. J Biol Chem 280:11528–11534. https://doi.org/10.1074/jbc.M413930200
60. Patel J, Du Y, Ard P et al (2004) The c-MYC oncoprotein is a substrate of the acetyltransferases hGCN5/PCAF and TIP60. Mol Cell Biol 24:10826–10834. https://doi.org/10.1128/MCB.24.24.10826-10834.2004
61. Perez-Perri JI, Dengler VL, Audetat KA et al (2016) The TIP60 complex is a conserved coactivator of HIF1A. Cell Rep 16:37–47. https://doi.org/10.1016/j.celrep.2016.05.082
62. Chen L, Fischle W, Verdin E, Greene W (2001) Duration of nuclear NF-kappa B action regulated by reversible acetylation. Science 293:1653–1657. https://doi.org/10.1126/science.1062374
63. Xiong Y, Guan K-L (2012) Mechanistic insights into the regulation of metabolic enzymes by acetylation. J Cell Biol 198:155–164. https://doi.org/10.1083/jcb.201202056
64. Ventura M, Mateo F, Serratosa J et al (2010) Nuclear translocation of glyceraldehyde-3-phosphate dehydrogenase is regulated by acetylation. Int J Biochem Cell Biol 42:1672–1680. https://doi.org/10.1016/j.biocel.2010.06.014
65. Hochachka P, Lutz P (2001) Mechanism, origin, and evolution of anoxia tolerance in animals. Comp Biochem Physiol B Biochem Mol Biol 130:435–459
66. Hochachka P, Rupert J, Monge C (1999) Adaptation and conservation of physiological systems in the evolution of human hypoxia tolerance. Comp Biochem Physiol A Mol Integr Physiol 124:1–17
67. Welinder C, Ekblad L (2011) Coomassie staining as loading control in western blot analysis. J Proteome Res 10:1416–1419. https://doi.org/10.1021/pr1011476
68. Storey K, Storey J (2004) Oxygen limitation and metabolic rate depression. In: Storey KB (ed) Functional Metabolism. Wiley, Hoboken, pp 415–442
69. Sauve A, Wolberger C, Schramm V, Boeke J (2006) The biochemistry of sirtuins. Annu Rev Biochem 75:435–465. https://doi.org/10.1146/annurev.biochem.74.082803.133500
70. Wijenayake S, Hawkins L, Storey K (2018) Dynamic regulation of six histone H3 lysine (K) methyltransferases in response to prolonged anoxia exposure in a freshwater turtle. Gene 649:50–57. https://doi.org/10.1016/J.GENE.2018.01.086
71. Wijenayake S, Storey K (2016) The role of DNA methylation during anoxia tolerance in a freshwater turtle (*Trachemys scripta elegans*). J Comp Physiol B 186:333–342. https://doi.org/10.1007/s00360-016-0960-x
72. Krivoruchko A, Storey K (2010) Epigenetics in anoxia tolerance: a role for histone deacetylases. Mol Cell Biochem 342:151–161. https://doi.org/10.1007/s11010-010-0479-5
73. Buck L, Land S, Hochachka P (1993) Anoxia-tolerant hepatocytes: Model system for study of reversible metabolic

suppression. Am J Physiol 265:49–56. https://doi.org/10.1152/ajpregu.1993.265.1.R49
74. Karmodiya K, Krebs A, Oulad-Abdelghani M et al (2012) H3K9 and H3K14 acetylation co-occur at many gene regulatory elements, while H3K14ac marks a subset of inactive inducible promoters in mouse embryonic stem cells. BMC Genomics 13:424. https://doi.org/10.1186/1471-2164-13-424
75. Huang J, Wan D, Li J et al (2015) Histone acetyltransferase PCAF regulates inflammatory molecules in the development of renal injury. Epigenetics 10:62–72. https://doi.org/10.4161/15592294.2014.990780
76. Wurtele H, Kaiser G, Bacal J et al (2012) Histone H3 lysine 56 acetylation and the response to DNA replication fork damage. Mol Cell Biol 32:154–172. https://doi.org/10.1128/MCB.05415-11
77. Biggar KK, Zhang J, Storey KB (2019) Navigating oxygen deprivation: liver transcriptomic responses of the red eared slider turtle to environmental anoxia. PeerJ. https://doi.org/10.7717/peerj.8144
78. Lee K, Workman J (2007) Histone acetyltransferase complexes: one size doesn't fit all. Nat Rev Mol Cell Biol 8:284–295. https://doi.org/10.1038/nrm2145
79. Kimura A, Matsubara K, Horikoshi M (2005) A decade of histone acetylation: marking eukaryotic chromosomes with specific codes. J Biochem 138:647–662. https://doi.org/10.1093/jb/mvi184
80. Ura K, Kurumizaka H, Dimitrov S et al (1997) Histone acetylation: Influence on transcription, nucleosome mobility and positioning, and linker histone-dependent transcriptional repression. EMBO J 16:2096–2107. https://doi.org/10.1093/emboj/16.8.2096
81. Hebbes T, Thorne A, Crane-Robinson C (1988) A direct link between core histone acetylation and transcriptionally active chromatin. EMBO J 7:1395–1402
82. Allfrey V, Faulkner R, Mirsky A (1964) Acetylation and methyalation of histones and their possible roles in the regulation of RNA synthesis. Proc Natl Acad Sci USA 51:786–794. https://doi.org/10.1073/pnas.51.5.786
83. Johnsson A, Durand-Dubief M, Xue-Franzen Y et al (2009) HAT-HDAC interplay modulates global histone H3K14 acetylation in gene-coding regions during stress. EMBO Rep 10:1009–1014. https://doi.org/10.1038/embor.2009.127
84. Xue-Franzen Y, Henriksson J, Burglin T, Wright A (2013) Distinct roles of the Gcn5 histone acetyltransferase revealed during transient stress-induced reprogramming of the genome. BMC Genomics 14:479. https://doi.org/10.1186/1471-2164-14-479
85. Barlev N, Poltoratsky V, Owen-Hughes T et al (1998) Repression of GCN5 histone acetyltransferase activity via bromodomain-mediated binding and phosphorylation by the Ku-DNA-dependent protein kinase complex. Mol Cell Biol 18:1349–1358
86. Lv L, Li D, Zhao D et al (2011) Acetylation targets the M2 isoform of pyruvate kinase for degradation through chaperone-mediated autophagy and promotes tumor growth. Mol Cell 42:719–730. https://doi.org/10.1016/j.molcel.2011.04.025
87. Kimura A, Horikoshi M (1998) Tip60 acetylates six lysines of a specific class in core histones in vitro. Genes Cells 3:789–800
88. Tang Y, Luo J, Zhang W, Gu W (2006) Tip60-dependent acetylation of p53 modulates the decision between cell-cycle arrest and apoptosis. Mol Cell 24:827–839. https://doi.org/10.1016/j.molcel.2006.11.021
89. Levine A (1997) p53, the cellular gatekeeper for growth and division. Cell 88:323–331. https://doi.org/10.1016/s0092-8674(00)81871-1
90. Maeda T, Hanna A, Sim A et al (2002) GADD45 regulates G2/M arrest, DNA repair, and cell death in keratinocytes following ultraviolet exposure. J Invest Dermatol 119:22–26. https://doi.org/10.1046/J.1523-1747.2002.01781.X
91. Vousden K, Ryan K (2009) p53 and metabolism. Nat Rev Cancer 9:691–700. https://doi.org/10.1038/nrc2715
92. Okoshi R, Ozaki T, Yamamoto H et al (2008) Activation of AMP-activated protein kinase induces p53-dependent apoptotic cell death in response to energetic stress. J Biol Chem 283:3979–3987. https://doi.org/10.1074/jbc.M705232200
93. Milne J, Denu J (2008) The sirtuin family: therapeutic targets to treat diseases of aging. Curr Opin Chem Biol 12:11–17. https://doi.org/10.1016/j.cbpa.2008.01.019
94. Finkel T, Deng C-X, Mostoslavsky R (2009) Recent progress in the biology and physiology of sirtuins. Nature 460:587–591. https://doi.org/10.1038/nature08197
95. Lai FMH, Miller AT (1973) Effect of hypoxia on brain and liver NAD+/NADH2 ratios in the fresh-water turtle (pseudemys scripta legans). Comp Biochem Physiol Part B Biochem 44:307–312. https://doi.org/10.1016/0305-0491(73)90367-2
96. Jackson DC, Ultsch GR (2010) Physiology of hibernation under the ice by turtles and frogs. J Exp Zool Part A Ecol Genet Physiol 313A:311–327. https://doi.org/10.1002/jez.603